

Plasmons in a superlattice with periodic defects

H. L. Cui

Department of Physics and Engineering Physics, Stevens Institute of Technology, Hoboken, New Jersey 07030

Godfrey Gumbs

Department of Physics, University of Lethbridge, Lethbridge, Alberta, Canada T1K 3M4

(Received 30 April 1990)

The plasmon excitation spectrum for a multiple-quantum-well superlattice with rectangular defect barriers in each quantum well is calculated in the random-phase approximation. It is demonstrated that both the intersubband and the intrasubband plasma frequencies can be effectively tuned subject to variations of the parameters characterizing the defect barrier in the quantum well, such as the barrier width, its height, and its position in the quantum well. For example, by varying the defect barrier width from 0 to about 40 Å, an order-of-magnitude increase is obtained in the intersubband plasma frequency, with corresponding changes in the intrasubband mode. It is shown that the variations of the collective excitation frequencies follow closely the electron energy subband structures and are therefore equally tunable via the defect barrier.

I. INTRODUCTION

The remarkable tailorability of subband structures of a semiconductor superlattice brought about by the introduction of either barriers in the quantum-well regions or potential wells in the barrier regions has recently been envisioned by Beltram and Capasso¹ and Peeters and Vasilopoulos.² These authors have demonstrated that the additional barriers (or wells) can effectively change the subband widths, as well as the energy gaps between the subbands. For example, an order-of-magnitude increase of the width of the lowest subband can be achieved as a result of varying the width of the positive potential barrier in the middle of the quantum well; moreover, an even greater change in the separation between the two lowest subbands is thus realized at the same time. In particular, when the *strength* of the additional barrier (defined to be the product of the barrier height times its width) matches the barrier strength of the original superlattice without defects, the energy gap between the two lowest subbands vanishes, reminiscent of the disappearance of band gaps along certain directions for a crystal with unit cells containing more than one identical atom.³ Whereas such a phenomenon is only "accidental" in nature for crystal lattices, it can be designed in the newly proposed superlattice structure. Virtually infinite possibilities exist for tuning the subband structures with the various combinations of the three parameters characterizing the additional barrier (well) at one's disposal: the height, the width, and the position of the barrier (well). From the crystal grower's standpoint, such a superlattice with a complex unit cell is well within the realm covered by today's growth techniques, such as molecular beam epitaxy (MBE). One such example, as proposed by Peeters and Vasilopoulos,² is based on the GaAs/Al_xGa_{1-x}As multiple-quantum-well superlattice. By increasing (either gradually or abruptly) the alloy composition (the value of x) in a confined region of the quantum well, a positive po-

tential barrier of desired shape can be created. A number of interesting applications taking advantage of the newly found tunability of the superlattice subbands have already been proposed, such as infrared-signal detecting,⁴ and surface-states tunneling.⁵ While the subband structure of a superlattice with complex unit cells is fairly well understood,^{1,2} its implications in the collective behavior of the electrons and in charge-transport processes in such structures remain unexplored. Of particular importance for experimental investigations such as far-infrared spectroscopy, light scattering, and fast-electron energy loss is the knowledge of the plasmon spectrum and its features associated with the complex unit cells. Specifically, it is expected that the plasma frequencies of both the intersubband modes and the intrasubband modes can be tuned by controlling the parameters characterizing the positive barrier or the negative well. In anticipation of the richness of the plasmon spectra in the superlattice with a complex unit cell, and to stimulate experimental interest, we have undertaken a theoretical investigation of the dielectric response and collective excitations of the new class of superlattice. In the remainder of this paper we report on our study in three parts. In Sec. II, we present the wave-number frequency-dependent dielectric function. The normal modes (plasmons), corresponding to the zeros of the dielectric response function, are studied in Sec. III. Concluding remarks and discussions of the special features of the predicted modes are presented in Sec. IV.

II. DIELECTRIC FORMULATION

Consider a superlattice grown along the z -direction with period l . Conduction electrons are free to move in the xy plane, but are subject to a periodic potential in the z direction. Single-electron states are described by a wave vector $\mathbf{k} = (\bar{k}, k_z)$, with $k = |\bar{k}| = (k_x^2 + k_y^2)^{1/2}$ and $-\pi/l < k_z < \pi/l$, as well as by a subband index n . The

electronic energy is defined by

$$E_{nk} = \frac{\hbar^2 k^2}{2m} + \varepsilon_{nk_z}, \quad (1)$$

where m is the electron effective mass, corresponding to the one-electron state

$$|n\mathbf{k}\rangle = \frac{1}{\sqrt{A}} e^{i\mathbf{k}\cdot\mathbf{x}} u_{nk_z}(z), \quad (2)$$

where A is a normalization area in the xy plane. The Bloch function $u_{nk_z}(z)$ can be obtained, e.g., with a Kronig-Penney-type procedure.

The dielectric-response function in the presence of a periodic potential was first discussed by Ehrenreich and Cohen,⁶ and later rederived by Wiser⁷ in a reciprocal-lattice representation. Similar approaches have also been used to treat semiconductor superlattices.⁸⁻¹⁰ Here, we will only present the result of the dielectric function of a superlattice with a complex unit cell. The derivation using the self-consistent-field method^{6,7} is a standard one, and it can be found elsewhere (Refs. 6-10). In the present case, for a system with periodic translational invariance with period l , the electronic polarizability, which relates the impressed potential to the induced charge density, and the dielectric function, which relates the self-consistent potential to the impressed potential, can be conveniently cast in matrix form with the reciprocal-lattice translation $G = 2n\pi/l$ ($n=0, \pm 1, \pm 2, \dots$) as their indices. Thus the longitudinal dielectric function is given by

$$\epsilon_{GG'}(\mathbf{q}, \omega) = \delta_{GG'} - v(\bar{q}, q_z + G) \Pi_{GG'}^{(0)}(\mathbf{q}, \omega), \quad (3)$$

with the Coulomb matrix element (κ is the high-frequency background dielectric constant)

$$v(\bar{q}, q_z + G) \equiv \frac{4\pi e^2}{\kappa[q^2 + (q_z + G)^2]}, \quad (4)$$

and the noninteracting electron density-density correlation function

$$\begin{aligned} \Pi_{GG'}^{(0)}(\mathbf{q}, \omega) &= \sum_{k_z, n, n'} \chi_{n, n'}^{(0)}(k_z, \mathbf{q}_z, \omega) I_{n, n'}^*(k_z, q_z, G) \\ &\quad \times I_{n, n'}(k_z, q_z, G). \end{aligned} \quad (5)$$

Here

$$I_{n, n'}(k_z, q_z, G) \equiv \int_0^l dz u_{nk_z}^*(z) e^{-iGz} u_{n'k_z + q_z}(z) \quad (6)$$

and

$$\chi_{n, n'}^{(0)}(k_z, \mathbf{q}_z, \omega) \equiv 2 \sum_k \frac{f(E_{n'\mathbf{k}+\mathbf{q}}) - f(E_{n\mathbf{k}})}{E_{n'\mathbf{k}+\mathbf{q}} - E_{n\mathbf{k}} + \hbar\omega + i0^+}, \quad (7)$$

where $f(E)$ is the Fermi-Dirac distribution function. Equation (7) is essentially the two-dimensional polarizability, but with the Fermi level shifted by the subband energy. At zero temperature the two-dimensional (2D) wave-vector integration can be performed analytically, leading to the real and imaginary parts similar to those of a strictly 2D electron sheet obtained by Stern¹¹

$$\begin{aligned} \text{Re}\chi_{n, n'}^{(0)}(k_z, \mathbf{q}_z, \omega) &= -\frac{m}{\pi q} \left[\Theta(E_F - \varepsilon_{n'k_z + q_z}) \left[\frac{q}{2} - \frac{m\omega'}{q} \text{sgn}(q^2 - 2m\omega') \Theta(Q_1^2 - k_{F1}^2) (Q_1^2 - k_{F1}^2)^{1/2} \right] \right. \\ &\quad \left. + \Theta(E_F - \varepsilon_{nk_z}) \left[\frac{q}{2} + \frac{m\omega'}{q} \text{sgn}(q^2 + 2m\omega') \Theta(Q_2^2 - k_{F2}^2) (Q_2^2 - k_{F2}^2)^{1/2} \right] \right], \end{aligned} \quad (8)$$

and

$$\text{Im}\chi_{n, n'}^{(0)}(k_z, \mathbf{q}_z, \omega) = -\frac{m}{\pi q} \left[\Theta(E_F - \varepsilon_{n'k_z + q_z}) \Theta(k_{F1}^2 - Q_1^2) (k_{F1}^2 - Q_1^2)^{1/2} - \Theta(E_F - \varepsilon_{nk_z}) \Theta(k_{F2}^2 - Q_2^2) (k_{F2}^2 - Q_2^2)^{1/2} \right], \quad (9)$$

where

$$\begin{aligned} \omega' &\equiv \omega + \varepsilon_{n'k_z + q_z} - \varepsilon_{nk_z}, \\ Q_1 &\equiv \frac{q}{2} - \frac{m\omega'}{q}, \quad Q_2 \equiv \frac{q}{2} + \frac{m\omega'}{q}, \\ k_{F1}^2 &\equiv 2m(E_F - \varepsilon_{n'k_z + q_z}), \quad k_{F2}^2 \equiv 2m(E_F - \varepsilon_{nk_z}), \end{aligned}$$

and E_F is the Fermi energy. Also $\Theta(x)$ is the Heaviside unit step function, and $\text{sgn}(x) \equiv \Theta(x) - \Theta(-x)$ is the sign function.

The collective modes are at the frequencies given by the roots of the determinantal equation

$$\det|\tilde{\epsilon}(\mathbf{q}, \omega)| = 0, \quad (10)$$

where the dielectric matrix is given by Eq. (3). Equation

(10) becomes intractable when the electrons are very much localized in the individual quantum wells, in which case many reciprocal-lattice vectors must be considered. However, if the electron wave functions within adjacent quantum wells overlap substantially, a quasi-three-dimensional treatment is more appropriate where only a few reciprocal-lattice vectors need be considered. In particular, in an experimental context, plasmons are detected at long wavelengths, using, e.g., far-infrared absorption, which corresponds to $q \ll 2\pi/l$ and $q_z \ll 2\pi/l$. Under these conditions the plasmon-dispersion relation simplifies to

$$1 - v(\bar{q}, q_z) \Pi_{00}^{(0)}(\mathbf{q}, \omega) = 0, \quad (11)$$

which can be readily solved to yield the frequencies of both the *intrasubband* and *intersubband* plasmons.

The system we choose to consider is the one treated by Peeters and Vasilopoulos,² which is a GaAs/Al_xGa_{1-x}As multiple-quantum-well superlattice with a defect barrier in each quantum well. One period of this structure is shown in Fig. 1. In this notation, the width of the well is w and that of each barrier separating two adjacent wells is b so that $l = b + w$. The electron effective mass is m_w^*, m_b^*, m_d^* inside the quantum well, the barrier and the defect, respectively. (The notation and values of the material parameters are the same as those used in Ref. 2.) The electron effective mass in the alloy Al_xGa_{1-x}As is given by $m/m_e = 0.067 + 0.083x$ and the barrier height is taken to be $V_0 = (0.693x + 0.222x^2)$ eV. We take $x = 0.3$ for the Al_xGa_{1-x}As in the barrier and $x = 0.4$ in the defect. The subband energy can be obtained in a straightforward way with the use of a transfer-matrix method for a Kronig-Penney potential problem.² This also yields the Bloch functions. However, the electronic wave functions obtained are hardly useful since they must be expressed as a product of transfer matrices and can only be represented via a numerical tabulation. In the present analysis for plasmon excitations we adopt an approximation scheme in which the single-particle energy is given by the Kronig-Penney calculation, while the single-particle wave functions are determined by considering only the first few Fourier components of the periodic superlattice potential, and the plasmon-dispersion relation we solve is given by Eq. (11).

Both the function $u_{nk_z}(z)$ and the superlattice potential $V(z)$ are periodic with the superlattice period l , whose Fourier expansions involve the reciprocal-lattice vectors only,

$$u_{k_z}(z) = \sum_G c(k_z - G) e^{-iGz} \quad (12)$$

and

$$V(z) = \sum_G V_G e^{iGz}. \quad (13)$$

Upon substituting Eqs. (12) and (13) into the single-electron Schrödinger equation, the problem reduces to

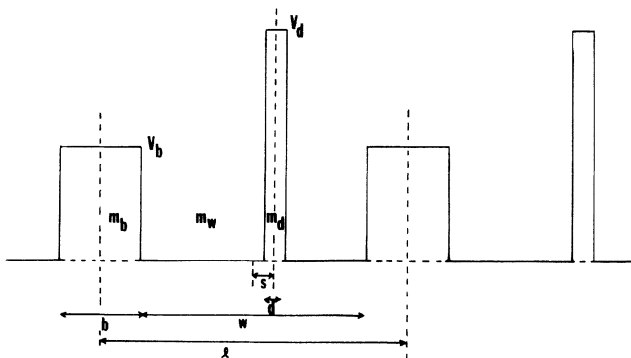


FIG. 1. Representation of the potential profile in a superlattice containing one defect barrier of width d . The center of the defect is at a distance s from the middle of the quantum well. The width of the quantum well is equal to w .

one of finding the Fourier coefficients $c(k_x - G)$. Retaining only the first three Fourier components of the superlattice potential, we obtain the wave functions

$$u_{nk_z}(z) = \frac{A_n(k_z)}{\sqrt{l}} [1 + \alpha_n^-(k_z) e^{-igz} + \alpha_n^+(k_z) e^{igz}], \quad (14)$$

where $g \equiv 2\pi/l$ is the shortest reciprocal-lattice vector;

$$\alpha_n^\pm(k_z) = \frac{V_g}{\epsilon_{nk_z} - (k_z \pm g)^2/2m - V_0}, \quad (15)$$

and $A_n(k_z)$ is a normalization factor given by

$$A_n(k_z) = [1 + \alpha_n^-(k_z)^2 + \alpha_n^+(k_z)^2]^{-1/2}. \quad (16)$$

The first three Fourier components of the superlattice potential are

$$V_0 = \frac{1}{l}(bV_b + dV_d), \quad (17)$$

and

$$V_g = V_{-g} = \frac{1}{\pi} \left[V_b \sin \left[\frac{bg}{2} \right] - V_d \sin \left[\frac{dg}{2} \right] \right]. \quad (18)$$

With this approximate wave function the form factor of Eq. (6) can be calculated in closed form. For example, the $G = 0$ -term is given by

$$I_{nn}(k_z, q_z, 0) = A_n(k_z) A_n(k_z + q_z) \times [1 + \alpha_n^-(k_z) \alpha_n^-(k_z + q_z) + \alpha_n^+(k_z) \alpha_n^+(k_z + q_z)]. \quad (19)$$

In the nearly-free-electron model, the band gap at the Brillouin-zone boundary is $2|V_g|$. Thus, from Eq. (18), the energy gap between the two lowest subbands vanishes when $V_b \sin(bg/2) = V_d \sin(dg/2)$. This approximation differs from the exact result $V_b b = V_d d$ by about 10% for the parameters we used in our calculations. The nearly-free-electron approximation is therefore fairly accurate in describing the plasmon spectrum of superlattices with periodic defects.

III. COLLECTIVE EXCITATIONS

The normal modes of the collective charge-density oscillations of the superlattice determined by the solutions of Eq. (10) fall into two categories: (a) those arising from virtual electronic transitions within a given miniband, to be referred to as intrasubband plasmons, and (b) those resulting from virtual electronic transitions between different minibands, called intersubband plasmons. In the case of a superlattice with a complex unit cell, both modes are frequency-tunable subject to variations of the parameters characterizing the additional barrier in the quantum well. In the following, we assume that the electron density is such that only the lowest subband is occupied initially, the Fermi level is always below the second subband. Thus there is only one intrasubband plasmon mode, involving electrons in the lowest subband. Amongst the many possible intersubband plasmon

branches we shall focus attention on the one involving the two lowest subbands.

In the long-wavelength limit ($ql \ll 1$), it can be shown^{8,9} that the intrasubband plasmon frequency is given by

$$\omega^2 = \omega_p^2 \sin^2 \Theta + \omega_g^2 \cos^2 \Theta, \quad (20)$$

where $\sin \Theta = q / (q^2 + q_z^2)^{1/2}$, $\cos \Theta = q_z / (q^2 + q_z^2)^{1/2}$, and $\omega_p^2 = 4\pi e^2 n_0 / \kappa m l$ is the square of the bulk plasma frequency (where n_0 is the areal density of the 2D electron gas) and

$$\omega_g^2 = \frac{4\pi e^2 n_0}{\kappa m_z l}. \quad (21)$$

The effective mass along the growth direction of the superlattice is defined by

$$\frac{1}{m_z} \equiv \frac{\sum_{\mathbf{k}} f(E_{1\mathbf{k}}) \frac{d^2 \epsilon_{1\mathbf{k}_z}}{dk_z^2}}{\sum_{\mathbf{k}} f(E_{1\mathbf{k}})}. \quad (22)$$

Thus the long-wavelength intrasubband plasmons depend crucially on the direction of propagation. For a plasmon propagating in the plane of the quantum well, its frequency is ω_p . On the other hand, for propagation along the growth direction of the superlattice the frequency is reduced to ω_g which is determined by the subband dispersion relation. For a flat (*dispersionless*) subband the effective mass $m_z \rightarrow \infty$, consequently $\omega_g \rightarrow 0$. In general, for an *oblique* direction of propagation, the resonance frequency is a hybridization of ω_p with ω_g , given by Eq. (20).

The long-wavelength limit of the intersubband plasma frequency approaches the subband separation as the wave vector approaches zero, but is nonetheless never exactly at the subband separation, due to the dispersion of the subbands. This is in contrast to the case of flat subbands where the intersubband plasmon matches the subband separation as the wave number approaches zero.

In demonstrating the dependence of the plasmon frequencies on the parameters describing the barrier in the quantum well of the superlattice, we choose to vary the barrier width d , while keeping the barrier height V_d and its position fixed. Specifically, we consider the case where the barrier is in the middle of the quantum well, i.e., $s=0$. Only with such a symmetric potential profile of the unit cell can a null band gap between the two lowest subbands be achieved.⁵

In Fig. 2, a set of solutions of the plasmon dispersion relation [Eq. (11)] as a function of the positive potential barrier widths are shown graphically. Both the intrasubband and the intersubband plasmon frequencies are seen to vary substantially as a function of the width of the defect barrier. In particular, the intersubband plasmon frequency is reduced from ~ 30 meV when the defect barrier is absent to ~ 3 meV for a defect barrier width of $d=38$ Å. An order-of-magnitude reduction in this mode frequency thus results. The lowest frequency of the intersubband plasmon (corresponding to $d=38$ Å) obtains

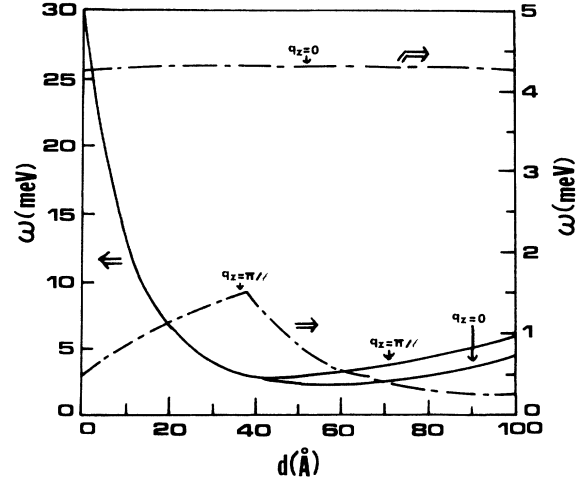


FIG. 2. Plot of the frequency of the plasmon modes [Eq. (11)] as a function of the positive potential barrier width d . We take $ql=0.1$ and $l=250$ Å, $b=50$ Å, $w=200$ Å, $s=0$, $V_d=313$ meV, $V_b=228$ meV, and $n_0=1.5 \times 10^{10}$ cm⁻². The values of the electron effective mass in the barrier and quantum-well regions are given in the text.

when the band gap vanishes at the Brillouin-zone boundary ($q_z = \pi/l$). For subbands with dispersion, the intersubband plasmon is broadened into a band, bounded at the top by the $q_z = \pi/l$ branch, and the branch having $q_z = 0$ at the bottom, for a given value of the wave number q . While such a bandwidth of the intersubband plasmon is barely discernible in the present case of small q ($qd=0.1$) for $d \leq 38$ Å, it becomes significant as d increases, reaching about 2 meV at $d=100$ Å.

The intrasubband plasmons are, like their intersubband

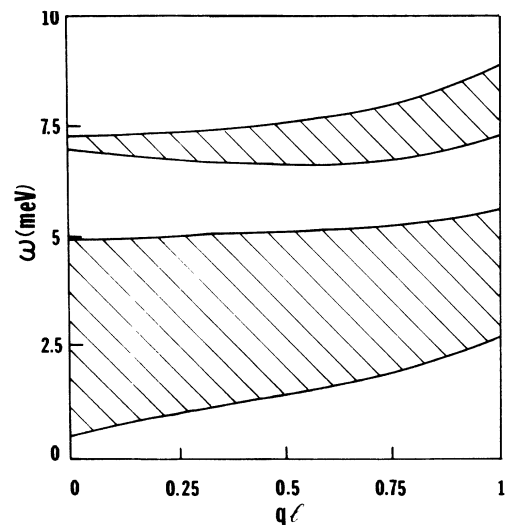


FIG. 3. The calculated plasmon modes as a function of wave number q for a defect barrier width $d=20$ Å, and electron density $n_0=2 \times 10^{10}$ cm⁻². Here the intersubband plasmon modes (top band) and the intrasubband plasmon band are separated by a gap of ~ 2 meV. The values used in the calculation for l , b , w , s , V_d , and V_b are given in the caption of Fig. 2.

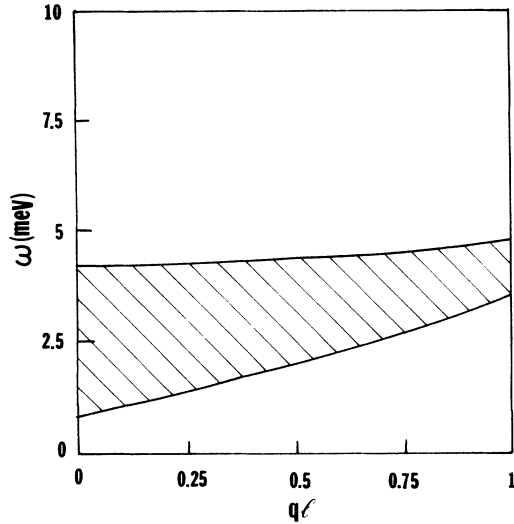


FIG. 4. Same as Fig. 3 but for $d = 40 \text{ \AA}$, and $n_0 = 1.5 \times 10^{10} \text{ cm}^{-2}$. The intersubband plasmon modes are contained within the intrasubband plasmon band. The values used in the calculation for l, b, w, s, V_b , and V_d are given in the caption of Fig. 2.

counterparts, broadened into a band in the presence of subband dispersion. However, unlike intersubband modes, the upper bound of this plasmon band corresponds to $q_z = 0$, and the lower bound has $q_z = \pi/l$. Whereas the $q_z = 0$ intrasubband frequency is insensitive to the variation of the defect barrier width, Fig. 2 clearly shows that the frequency of the $q_z = \pi/l$ mode at first increases as d increases, reaching a maximum at $d = 38 \text{ \AA}$, then decreases as d is further increased. Such a sharp contrast in the d dependences of the two frequencies (corresponding to $q_z = 0$ and $q_z = \pi/l$) serves to remind one of the difference in the nature of the collective charge-

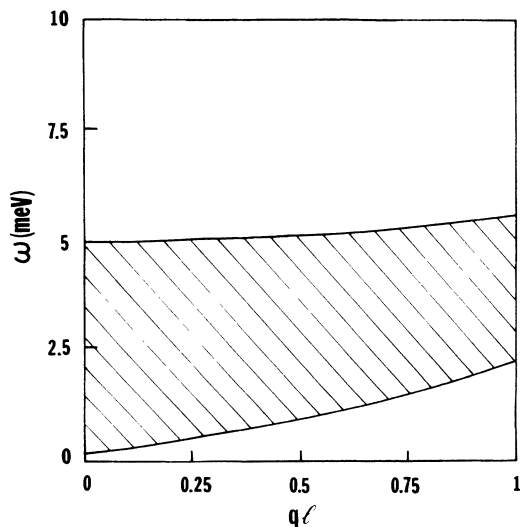


FIG. 5. Same as Fig. 3 but for $d = 60 \text{ \AA}$, and $n_0 = 2 \times 10^{10} \text{ cm}^{-2}$. The intersubband plasmon modes are contained within the intrasubband plasmon band. The values used in the calculation for l, b, w, s, V_b , and V_d are given in the caption of Fig. 2.

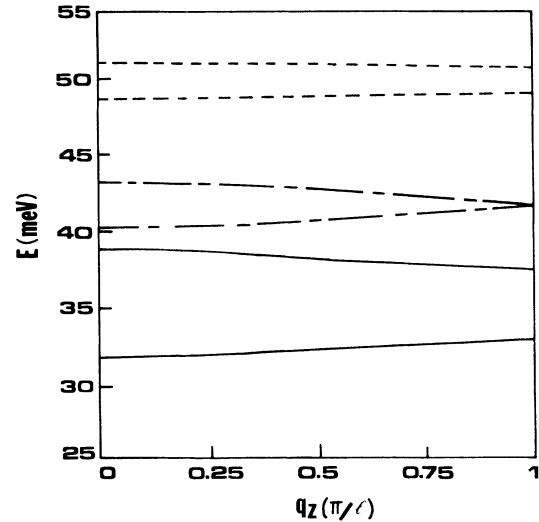


FIG. 6. The two lowest subbands for the three values of defect width d presented in Figs. 3–5 are plotted as a function of the wave number q_z . The values used in the calculation for l, b, w, s, V_b , and V_d are given in the caption of Fig. 2. Solid lines: $d = 20 \text{ \AA}$; chain lines: $d = 40 \text{ \AA}$; dotted lines: $d = 60 \text{ \AA}$.

density oscillations along the superlattice growth direction and perpendicular to it: the former is a direct consequence of the delocalization of electrons from the individual quantum wells which leads to a finite subband width, hence finite electron effective mass along the growth direction. Such a close correspondence with the subband width makes the collective oscillation along the growth direction equally controllable as the subband width. Furthermore, like the subband width, this collective mode is sensitive to the detailed composition of the superlattice unit cell. On the other hand, the collective charge-density oscillation in the plane of the quantum well involves in-plane electronic motion (which is free-electron-like irrespective of the superlattice unit-cell structure) only, with frequencies essentially fixed by the 2D electron density and the superlattice period.

While Fig. 2 shows plasma frequencies for a small and fixed q value, the general dependence on the wave number q for several representative values of d are shown in Figs. 3–5. For a defect barrier width $d = 20 \text{ \AA}$, the plasmon dispersion is plotted in Fig. 3. Here the intersubband plasmon modes (top band) and the intrasubband (bottom band) plasmon band are separated by a gap of $\sim 2 \text{ meV}$. Thus they should be clearly distinguishable experimentally. However, such a distinction is lost for larger values of d . At $d = 40$ and 60 \AA , shown in Figs. 4 and 5, respectively, the intersubband plasmon modes are contained within the intrasubband plasmon band, and can no longer be separated from the latter. These changes in the plasmon dispersion relation follow closely the variations in the subband widths and subband separation. To illustrate the close correspondence between the subband structures and the collective excitation spectrum we show in Fig. 6 the two lowest subbands for the three values of d considered in Figs. 3–5 as functions of the wave number q_z . It is clear on examination of the plasma

dispersion relations presented in Figs. 3–5 in conjunction with Fig. 6 that almost all the salient features of the former can be traced to the structure of the subbands. This also justifies the use of the approximate Bloch functions, since it is the single-electron energy that plays the most important role in the determination of the collective behavior of the electrons.

IV. CONCLUSIONS

In summary, we have discussed collective charge-density fluctuations in a semiconductor superlattice with periodic defect barriers located in the quantum wells, and have examined the dependence of the plasmon spectra on the characteristics of the defect barriers. It is demonstrated that by simply varying the defect barrier width from 0 to about 40 Å, one can bring about an order of magnitude change in the intersubband plasmon frequency, and similar changes in the intrasubband plasmon frequency, which points to the possibility of tailor-made plasma frequencies in this unique class of semiconductor superlattices. In view of the important technical advantages this new class of semiconductor superlattices have to offer over conventional superlattice structures, and the impending applications such as in infrared detectors and tunneling devices, a clear understanding of the collective behavior of the electrons in these novel structures is necessary in both the evaluation of device performance

and further exploration via such standard techniques as infrared spectroscopy, light scattering, and fast-electron energy loss. Our work represents a first step toward such an understanding, and in presenting it we hope to stimulate further theoretical and experimental interest in this problem. The predicted plasma spectra of the “defective” multiple-quantum-well superlattice should be observable with any of the above mentioned techniques. In this regard the intersubband mode for small defect barrier widths is especially promising since it is not Landau-damped at long wavelengths ($qd < 1$), and is far removed from the intrasubband mode. In contrast the lower branch of the intrasubband plasmon is not clearly separated from the single-particle excitation, and is therefore subject to Landau damping. For larger defect barrier widths the intersubband mode is submerged in the intrasubband plasma spectrum, and it will be interesting to see experimentally whether the two resonant frequencies will show up as separate signals or as a mixture of the two.

ACKNOWLEDGMENTS

The authors are grateful to Dr. J. Yang for participation in the early stage of this work, and to Professor N. J. M. Horing for useful discussions. One of us (G.G.) acknowledges partial financial support by the Natural Sciences and Engineering Research Council of Canada.

¹F. Beltram and F. Capasso, *Phys. Rev. B* **38**, 3580 (1988).

²F. M. Peeters and P. Vasilopoulos, *Appl. Phys. Lett.* **55**, 1106 (1989).

³C. Kittel, *Introduction to Solid State Physics*, 6th ed. (Wiley, New York, 1986).

⁴W. Trzeciakowski and B. D. McCombe, *Appl. Phys. Lett.* **55**, 891 (1989).

⁵G. Gumbs and A. Salman, *Phys. Rev. B* **41**, 10 124 (1990).

⁶H. Ehrenreich and M. H. Cohen, *Phys. Rev.* **115**, 786 (1959).

⁷N. Wiser, *Phys. Rev.* **129**, 62 (1963).

⁸H. Ishida, *J. Phys. Soc. Jpn.* **55**, 4396 (1986).

⁹X. L. Lei, R. Q. Yang, and C. H. Tsai, in *Physics of Superlattices and Quantum Wells*, edited by C. H. Tsai *et al.* (World Scientific, Singapore, 1989).

¹⁰X. D. Zhu, X. Xia, J. J. Quinn, and P. Hawrylak, *Phys. Rev. B* **38**, 5617 (1988).

¹¹F. Stern, *Phys. Rev. Lett.* **18**, 546 (1967).